

Resonant-cavity-induced phase locking and voltage steps in a Josephson array

E. Almaas* and D. Stroud†

Department of Physics, The Ohio State University, Columbus, Ohio 43210

(Received 14 December 2000; published 22 March 2001)

We describe a simple dynamical model for an underdamped Josephson junction array coupled to a resonant cavity. From numerical solutions of the model in one dimension, we find that (i) current-voltage characteristics of the array have self-induced resonant steps (SIRS), (ii) at fixed disorder and coupling strength, the array locks into a coherent, periodic state above a critical number of active Josephson junctions, and (iii) when N_a active junctions are synchronized on an SIRS, the energy emitted into the resonant cavity is quadratic with N_a . All three features are in agreement with a recent experiment [P. Barbara, A. B. Cawthorne, S. V. Shitov, and C. J. Lobb, Phys. Rev. Lett. **82**, 1963 (1999)].

DOI: 10.1103/PhysRevB.63.144522

PACS number(s): 05.45.Xt, 05.45.-a, 74.40.+k

I. INTRODUCTION

Arrays of Josephson junctions have long been studied both experimentally¹ and theoretically² as a potentially controllable source of microwave radiation. Most studies have been carried out on overdamped junction arrays with external loads. Typically, a dc current is injected into the array, producing ac voltage oscillations in each of the junctions. If all the junctions are locked to the same frequency, then the radiated power should vary as the square of the number of junctions. Overdamped junctions are usually studied, because underdamped junctions can exhibit hysteresis and chaotic behavior. However, even overdamped arrays have proven difficult to synchronize: their largest experimentally achieved dc to ac conversion efficiency is only about 1%.³

Recently, Barbara *et al.*⁴ achieved a 17% degree of power conversion in an *underdamped* two-dimensional array placed within a resonant electromagnetic cavity. In this case, the synchronization was achieved by an indirect coupling between each junction and the electromagnetic field of the cavity mode. The results were characterized by striking threshold behavior: typically no synchronization was achieved for arrays shorter than a certain threshold number of junctions.

In this article, we present and numerically study a simple model for the dynamics of an underdamped Josephson junction array coupled to a resonant cavity. This model generalizes one used recently to describe the energetics of such a system.⁵ It bears many resemblances to previous dynamical models, which either connect this array to laser action in excitable two-level atoms⁶ or introduce various types of impedance loads to provide global coupling between junctions.⁷⁻¹⁰ In our model, however, we infer the equations of motion starting from a more conventional Hamiltonian which describes Josephson junctions coupled to a vector potential.¹¹ Even though our model is only one-dimensional, our results show many of the features seen experimentally in two-dimensional arrays,⁴ including (i) mode locking into a coherent state above a critical number N_c of active junctions, (ii) a quadratic dependence of the energy on the number of active junctions above N_c , and (iii) most strikingly, self-induced steps at voltages corresponding to multiples of the cavity frequency. Thus, the results suggest that suitably de-

signed experiments on one-dimensional arrays might produce similar results to those seen in two dimensions.

The remainder of this paper is organized as follows. In Sec. II, we present our model Hamiltonian. Section III gives our numerical results, and Sec. IV gives some brief concluding remarks.

II. MODEL

We begin with the following Hamiltonian model for a one-dimensional array of N Josephson junctions placed in a resonant cavity, which we assume supports only a single photon mode of frequency Ω :

$$\begin{aligned} H &= H_{\text{photon}} + H_C + H_J \\ &= \hbar\Omega \left(a^\dagger a + \frac{1}{2} \right) + \sum_{j=1}^N E_{C_j} n_j^2 - \sum_{j=1}^N E_{J_j} \cos(\gamma_j). \end{aligned} \quad (1)$$

Here, H_{photon} is the energy contained in the photon mode of the cavity, H_C is the capacitive energy, and H_J is the Josephson energy of the array. a^\dagger and a are photon creation and annihilation operators, $E_{C_j} = q^2/(2C_j)$ is the approximate capacitive energy of a single junction, and $E_{J_j} = \hbar I_{C_j}/q$ is the Josephson coupling energy of a junction (where C_j is a capacitance, I_{C_j} a critical current, and $q = 2|e|$ is the Cooper pair charge). Finally, $\gamma_j = \phi_j - [(2\pi)/\Phi_0] \int_j \mathbf{A} \cdot d\mathbf{s} \equiv \phi_j - A_j$ is the gauge-invariant phase difference across a junction, where ϕ_j is the phase difference across a junction in the absence of the vector potential \mathbf{A} , $\Phi_0 = hc/q$ is the flux quantum, and the line integral is taken across the junction.

We assume that \mathbf{A} arises from the electromagnetic field of the normal mode of the cavity. In Gaussian units, this vector potential is given by^{12,13} $\mathbf{A}(\mathbf{x}, t) = \sqrt{(hc^2)/(2\Omega)} (a(t) + a^\dagger(t)) \mathbf{E}(\mathbf{x})$; here $\mathbf{E}(\mathbf{x})$ is the electric field of the mode, normalized so that $\int_V d^3x |\mathbf{E}(\mathbf{x})|^2 = 1$, V being the system volume. Similarly,¹³ $A_j = \sqrt{g_j} (a + a^\dagger)$, where

$$g_j = \frac{\hbar c^2}{2\Omega} \frac{(2\pi)^3}{\Phi_0^2} \left[\int_j \mathbf{E}(\mathbf{x}) \cdot \mathbf{ds} \right]^2 \quad (2)$$

is an effective coupling constant describing the interaction between the junction and the cavity.

The time-dependence of the operators a , a^\dagger , n_i , and ϕ_i follows from Eq. (1) together with the Heisenberg equations of motion $i\hbar\dot{\mathcal{O}} = [\mathcal{O}, H]$, where $[\dots, \dots]$ is a commutator and \mathcal{O} an operator. In order to evaluate these equations of motion, we use the relations $[a, a^\dagger] = 1$, $[a, a] = [a^\dagger, a^\dagger] = 0$, and $[n_j, \pm \phi_k] = \mp i\delta_{jk}$, with other commutators set equal to zero; we also make use of the operator relation $[A, F(B)] = [A, B]F'(B)$ for any function $F(B)$ of an operator B .

To simplify the resulting equations, we introduce the notation $a = a_R + ia_I$ and $\omega_{pj}^2 = 2\omega_{Cj}\omega_{Jj}$, where $\omega_{Cj} = E_{Cj}/\hbar$ and $\omega_{Jj} = E_{Jj}/\hbar$. We also define a dimensionless natural time $\tau = \bar{\omega}_p t$, where $\bar{\omega}_p$ is a suitable average value of ω_{pj} . For numerical convenience, we assume that g_j has the same value g for each junction (this is plausible in the long-wavelength limit where the electric field varies on a scale large compared to the array size). Then, after some algebra, the equations of motion can be cast into the form $\dot{\phi}_j - \tilde{n}_j = 0$, $\dot{\tilde{n}}_j + (\omega_{pj}^2/\bar{\omega}_p^2)\sin(\phi_j - 2\tilde{a}_R) = 0$, $\dot{\tilde{a}}_R - \tilde{\Omega}\tilde{a}_I = 0$, and $\dot{\tilde{a}}_I + \tilde{\Omega}\tilde{a}_R - g\sum_j(\omega_{Jj}/\bar{\omega}_p)\sin(\phi_j - 2\tilde{a}_R) = 0$. Here the dot represents a derivative with respect to τ , and we have introduced the new variables $\tilde{a}_R = \sqrt{g}a_R$, $\tilde{a}_I = \sqrt{g}a_I$, $\tilde{n}_j = (2\omega_{Cj}/\bar{\omega}_p)n_j$, and $\tilde{\Omega} = \Omega/\bar{\omega}_p$.

As stated above, these equations describe the time evolution of various operators, not all of which commute with one another. Furthermore, they do not include either damping or a driving current. In order to make these equations amenable to numerical computation, we therefore replace the operators by c -numbers. This procedure should be reasonable when the eigenvalues of $n_j \gg 1$.⁶ We can include the important effects of dissipation within a Hamiltonian formalism by coupling each phase degree of freedom to a separate collection of harmonic oscillators with a suitable spectral density, as has been discussed by Chakravarty *et al.*¹⁴ Specifically, we may add a term to H of the form $\sum_{j=1}^N [\phi_j \sum_{\alpha} f_{\alpha}^{(j)} x_{\alpha}^{(j)} + \sum_{\alpha} ((1/2m_{\alpha})(p_{\alpha}^{(j)})^2 + (m_{\alpha}/2)\omega_{\alpha}^2 x_{\alpha}^{(j)2})]$, where the $f_{\alpha}^{(j)}$ are appropriate coupling constants, and $x_{\alpha}^{(j)}$ and $p_{\alpha}^{(j)}$ are the canonically conjugate harmonic oscillator variables. If the spectral density of the harmonic oscillators $J_j \equiv (\pi/2)\sum_{\alpha} [(f_{\alpha}^{(j)})^2/m_{\alpha}\omega_{\alpha}] \delta(\omega - \omega_{\alpha}) = (\hbar/2\pi)\alpha_j|\omega|\theta(\omega_c - \omega)$, where ω_c is a cutoff frequency comparable to a typical phonon frequency, $\alpha_j = R_0/R_j$, and $R_0 = h/(2e)^2$, then it can be shown that the dissipation is ohmic.^{14,15} Integrating out the variables $x_{\alpha}^{(j)}$ and $p_{\alpha}^{(j)}$ then leads to the usual resistively-shunted junction equation¹⁶ with ohmic damping corresponding to a shunt resistance R_j . A driving current can be included similarly in the Hamiltonian formalism by adding to H a ‘‘washboard potential’’ of the form $(\hbar I/q)\sum_{j=1}^N \phi_j$.

These modifications lead to the following equations of motion for the $2N+2$ variables ϕ_i , n_i , a_R , and a_I :

$$\dot{\phi}_j = \tilde{n}_j,$$

$$\dot{\tilde{n}}_j = \frac{I}{I_c(1+\Delta_j)} - \frac{1}{Q_j}\tilde{n}_j - \sin(\phi_j - 2\tilde{a}_R), \quad (3)$$

$$\dot{\tilde{a}}_R = \tilde{\Omega}\tilde{a}_I,$$

$$\dot{\tilde{a}}_I = -\tilde{\Omega}\tilde{a}_R + \tilde{g}\sum_j (1+\Delta_j)\sin(\phi_j - 2\tilde{a}_R).$$

Here, we have redefined the effective coupling as $\tilde{g} = g\omega_{Jj}/\bar{\omega}_p$, and introduced a damping coefficient $Q_j = \bar{\omega}_p R_j C_j$, where R_j is the shunt resistance. We also introduce a disorder parameter $\Delta_j = (I_{cj} - I_c)/I_c$, where I_c is a suitable average critical current. In writing these equations, we have also made the simplifying assumption that both $C_j R_j$ and I_{cj}/C_j are independent of j , so that each junction has the same damping coefficient Q_j . The equations of motion include no dissipation due to the cavity walls, though this effect could readily be included similarly via a cavity Q factor. Note that the first two equations in Eq. (3) reduce to the RCSJ model in the limit of no coupling to the cavity ($\tilde{g} = 0$), and the last two equations to those of a harmonic oscillator with eigenfrequency $\tilde{\Omega}$.

III. NUMERICAL RESULTS

We have solved Eqs. (3) for the variables n_i , ϕ_i , \tilde{a}_R , and \tilde{a}_I numerically by implementing the adaptive Bulirsch-Stoer method, which is both fast and accurate.¹⁷ We choose I_{cj} , for each junction, j , randomly and independently from a uniform distribution between $I_c(1-\Delta)$ and $I_c(1+\Delta)$, where Δ is a measure of the disorder, but for convenience we assume that \tilde{g} is independent of j . We initialize the simulations with all the phases randomized between $[0, 2\pi]$, and $a_R = a_I = n_j = 0$. We then let the system equilibrate for a time interval $\Delta\tau = 10^4$, after which we evaluate averages over a time interval $\Delta\tau = 2 \times 10^3$, using 2^{16} evenly spaced sampling points.

In Fig. 1, we show the current-voltage characteristics for $N = 40$ junctions with $\Delta = 0.05$ and $\tilde{g} = 0.001$, evaluating the time-averaged voltage from the Josephson relation, $\langle V \rangle = [1/Q_j] \langle \sum_{j=1}^N \dot{\gamma}_j \rangle$. A striking feature of this plot is the *self-induced resonant steps* (SIRS), at which $\langle V \rangle$ remains approximately constant over a range of applied current. The most prominent step occurs at $\langle V \rangle / (NRI_c) = \tilde{\Omega}/Q_j$, but there is another, less obvious, step at $2\tilde{\Omega}/Q_j$. We believe the steps occur at all $(m/n)\tilde{\Omega}/Q_j$, where m and n are integers, as further discussed below. Similar steps were seen experimentally in a *two-dimensional* array of underdamped Josephson junctions coupled to a resonant cavity.⁴ The present results suggest that similar steps may also be observable even in experiments on one-dimensional arrays.

When we solve the system of equations (3) numerically

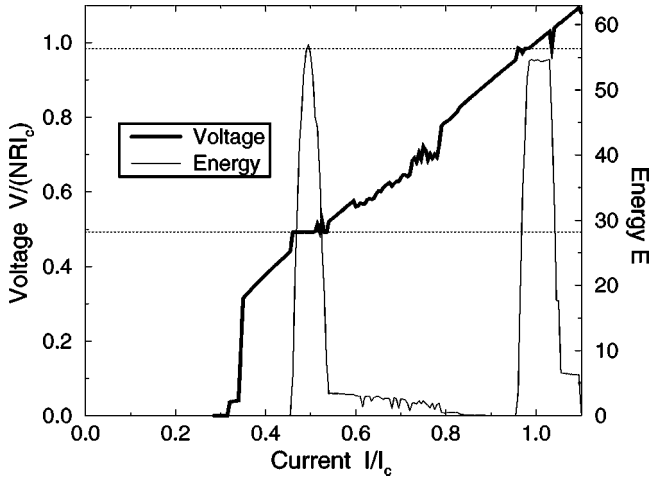


FIG. 1. Left scale: Current-voltage (IV) characteristics for an underdamped Josephson array of $N=40$ junctions and system parameters $\tilde{\Omega}=2.2$, $Q_J=\sqrt{20}$, $\Delta=0.05$, and $\tilde{g}=0.001$, as defined in the text. Right-hand scale: total photon energy in the cavity $\bar{E}=(\bar{a}_R^2+\bar{a}_I^2)$. Predicted voltages for the integer self-induced resonant steps (SIRS) are shown as dotted lines.

for a single junction, we find SIRS for fractions $(n/m)=1, 4/3, 3/2, 5/3, 2, 5/2, 3, 4, \dots$. The step width in current is very sensitive to \tilde{g} , and, indeed, we have thus far found the steps only for a limited range of \tilde{g} . For the larger, disordered arrays, we have not yet seen the fractional SIRS.

Figure 1 also shows the time-averaged total energy $\bar{E}=(\bar{a}_R^2+\bar{a}_I^2)$ as a function of I/I_c for the same array. The total energy in the cavity increases dramatically when the array is on a SIRS, and is very small otherwise. This sharp increase signals the onset of coherence within the array, as further discussed below.

Figure 2 shows the calculated voltage power spectrum $P(\omega)=|\int_{-\infty}^{\infty} V_{tot}(\tau)\exp(i\omega\tau)d\tau|^2$, for two values of the driving current: $I/I_c=\tilde{\Omega}/Q_J$ [Figs. 2(a) and 2(b)] and $I/I_c=0.9$ [Figs. 2(c) and 2(d)]; all other parameters are the same as in Fig. 1. In Fig. 2(a), all the junctions are on the first SIRS and the power spectrum has peaks at the cavity frequency $\tilde{\Omega}$ and its harmonics. In Fig. 2(c), the array is tuned off the step. The power spectrum shows that the array is not synchronized in this case; instead, the individual junctions oscillate approximately at their individual resonant frequencies and their harmonics and subharmonics. In Figs. 2(b) and 2(d), we show the same case as in Fig. 2(a) and 2(c), respectively, except that the coupling constant, \tilde{g} , is artificially set equal to zero. In this case, the junctions are, of course, independent of one another, and the result is that of a disordered one-dimensional Josephson array with no coupling between the junctions.

Next, we turn to the dependence of these properties on the number of active junctions, N_a , in the array. The concept of active junction number, in the terminology of Ref. 9, is meaningful only for underdamped junctions. As is well known, an underdamped junction is bistable and hysteretic in certain ranges of current, and can have either zero or a finite

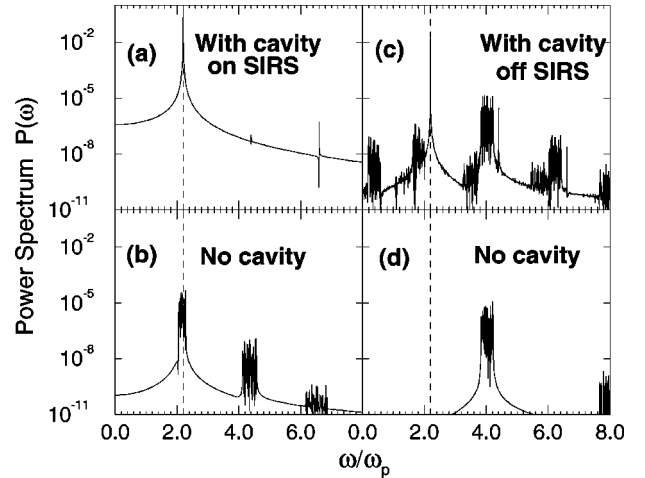


FIG. 2. Power spectrum, $P(\omega)$, of the ac voltage across the array, plotted versus frequency, ω , at two driving currents: (a) and (b) $I/I_c=0.492$, corresponding to the first integer SIRS, and (c) and (d) $I/I_c=0.90$, slightly off a SIRS. Other parameters are the same as in Fig. 1. (b) and (d) are the same as (a) and (c) except that the effective coupling to the resonant cavity is $\tilde{g}=0$. The vertical dashed line shows the resonant frequency of the cavity.

time-averaged voltage across it, depending on the initial conditions. In the present case, N_a denotes the number of junctions (out of N total) which have a finite time-averaged voltage drop. We can tune N_a by suitably choosing the initial conditions, ϕ_i and $\dot{\phi}_i$, for each junction.⁹

We have studied the properties of the disordered array ($\Delta=0.10$) for $N=40$ junctions, and a driving current $I/I_c=\tilde{\Omega}/Q_J$. This current not only lies well within the bistable region, but also leads to a voltage on the first integer SIRS. The total, time-averaged energy of the cavity, $\bar{E}(N_a)$ [normalized to $\bar{E}(6)$] is plotted as a function of N_a in Fig. 3. The active junctions are unsynchronized up to a threshold value $N_c=15$. Above this value, \bar{E} increases as a quadratic function of N_a , i.e., $\bar{E}=c_0+c_1N_a+c_2N_a^2$, where c_0 , c_1 , and c_2 are constants (full line in Fig. 3). By contrast, \bar{E} is approximately independent of N_a for $N_a<N_c$. At $N_a=N_c$, there is a discontinuous jump in \bar{E} by approximately a factor of 3 (see inset to figure). A similar quadratic dependence above a synchronization threshold was also seen in Ref. 4, though for a two-dimensional array in an applied weak magnetic field. By contrast, if the system is in the bistable region, but *not* tuned to a self-induced resonant step, \bar{E} does *not* increase quadratically with N_a . Instead, we find $\bar{E}(N_a)$ exhibits a series of plateaus separated by discontinuous jumps (not shown in the figure).

To measure the degree of synchronization among the Josephson junctions, we plot the Kuramoto order parameter,¹⁹ $\langle r \rangle$ for the same parameters, as a function of number of active junctions, N_a , (right-hand scale in Fig. 3). $\langle r \rangle$ is defined by $\langle r \rangle = \langle |(1/N_a)\sum_{j=1}^{N_a} \exp(i\phi_j)| \rangle_\tau$, where $\langle \dots \rangle_\tau$ denotes a time average. Note that $\langle r \rangle=1$ represents perfect synchronization among the active junctions, while $\langle r \rangle=0$

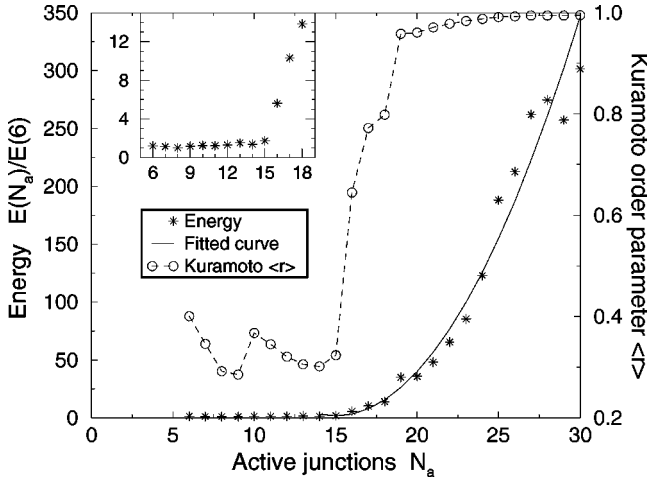


FIG. 3. Left-hand scale and asterisks: Photon energy \bar{E} in the resonant cavity when the array is current driven on a SIRS, plotted versus number of active junctions, N_a . The array parameters are $N=40$, $\tilde{\Omega}=2.2$, $Q_J=\sqrt{20}$, $\Delta=0.10$, $\tilde{g}=0.001$, and $I/I_c=\tilde{\Omega}/Q_J$ (see text). Full curve shows the best fit of \bar{E} to the function $c_2 N_a^2 + c_1 N_a + c_0$ for $N_a > 15$, the threshold for synchronization. Inset: $\bar{E}(N_a)$ near $N_a=15$, showing jump near synchronization threshold. Right-hand scale and open circles: Kuramoto order parameter, $\langle r \rangle$ (see text), for the same array. Dots connecting circles are guides to the eye. The sharp increase in $\langle r \rangle$ and the quadratic increase in \bar{E} both start near $N_a=15$.

would correspond to no correlations between the different phase differences, ϕ_i . As is clear from Fig. 3, there is an abrupt increase in $\langle r \rangle$ at $N_a=N_c$, indicative of a *dynamical transition* from an unsynchronized to a synchronized state, as N_a is increased past a critical value, while other parameters are kept fixed. As expected from similar transitions in other models,²⁰ this transition is not inhibited by the finite disorder in the I_c 's. Note that $\langle r \rangle$ approaches unity for large N_a , representing perfect synchronization. This transition is the dynamic analog of that analyzed by an equilibrium mean-field theory in Ref. 5.

IV. DISCUSSION

We now briefly discuss the physics behind the present numerical results. At present, although these results agree in many respects with experiment, we can give only some rough intuitive arguments why these results emerge from our equations of motion.

First, the existence of a transition from incoherence to coherence, as a function of the number of active junctions N_a , is undoubtedly a consequence of the ‘‘mean-field-like’’ nature of the interaction between the junctions and the cavity. Specifically, because each junction is effectively coupled to every other junction via the cavity, the strength of the coupling increases with N_a . Thus, a transition to coherence is to be expected for sufficiently large N_a . A similar argument was made in the equilibrium case in Ref. 5.

The self-induced resonant steps can also be understood on the basis of a simple intuitive argument. Basically, as noted in Ref. 4, these steps are the analogs of Shapiro steps in

conventional Josephson junctions, and occur, we believe, for a similar reason. Namely, when a current is applied to a junction, it produces a time-dependent response in \tilde{a}_R , setting it into motion at the natural oscillation frequency of the cavity, $\tilde{\Omega}$. This oscillation then acts back on the junction like an ac current, so that the junctions experience the combined effects of a dc and an ac current. This combination produces constant-voltage steps in the junction, just as in a conventional junction.

This argument can be made a little more precise if we consider the time-dependent response of \tilde{a}_R when a voltage is applied to the junction. We write this response as $\tilde{a}_R = \tilde{a}_0 \cos(\tilde{\Omega}\tau + \alpha_0) + \tilde{a}_1 \sin(Q_J V \tau + \alpha_1)$, where \tilde{a}_i and α_i are constants. The Josephson current through the junction is then $I_c \sin(\phi - 2\tilde{a}_R)$. If we substitute the above form for \tilde{a}_R into the expression for the current, and use standard expansions for quantities of the form $\sin(A + B \cos(\beta\tau))$ in terms of Bessel functions,¹⁸ we find that there is a nonzero dc current whenever $Q_J V = (n/m)\tilde{\Omega}$, where n and m are integers. This condition is similar to that for the occurrence of a Shapiro step in a conventional Josephson junction driven by a combined dc and ac voltage. The results of Fig. 1 show that at least the integer steps can be seen within the model of Eqs. (3) for a suitable choice of junction and cavity parameters.

Finally, we speculate about the reasons for the occurrence of the SIRS even in one-dimensional arrays. The arguments given above suggest that the occurrence of such resonances should not depend on the dimensionality of the array, but only on the existence of a suitable induced ac drive. Indeed, an experimental observation of such steps in 1D arrays has recently been reported,²¹ consistent with the present model.

In summary, we have presented a model for a one-dimensional array of underdamped Josephson junctions coupled to a resonant cavity. We have studied the classical limit of the Heisenberg equations of motion for this model, valid in the limit of large numbers of photons, and included damping by coupling each phase difference to an ohmic heat bath. In the presence of a dc current drive, we find numerically that (i) the array exhibits self-induced resonant steps (SIRS), similar to Shapiro steps in conventional arrays; (ii) there is a transition between an unsynchronized and a synchronized state as the number of active junctions is increased while other parameters are held fixed; and (iii) when the array is biased on the first integer SIRS, the total energy increases quadratically with number of active junctions. All these features appear consistent with experiment.⁴ Further study is underway in order to ascertain whether or not these features remain true of two-dimensional arrays and with gauge-invariant damping.

ACKNOWLEDGMENTS

We are grateful for support from NSF Grant No. DMR97-31511. Computational support was provided by the Ohio Supercomputer Center, and the Norwegian University of Science and Technology (NTNU). We thank C. J. Lobb and R. V. Kulkarni for useful conversations.

*Electronic address: Almaas.1@osu.edu

†Electronic address: stroud@mps.ohio-state.edu

- ¹See, e.g., P. A. A. Booij and S. P. Benz, *Appl. Phys. Lett.* **68**, 3799 (1996); S. Han, B. Bi, W. Zhang, and J. E. Lukens, *ibid.* **64**, 1424 (1994); V. K. Kaplunenko, J. Mygind, N. F. Pedersen, and A. V. Ustinov, *J. Appl. Phys.* **73**, 2019 (1993); K. Wan, A. K. Jain, and J. E. Lukens, *Appl. Phys. Lett.* **54**, 1805 (1989).
- ²See, e.g., K. Wiesenfeld, S. P. Benz, and P. A. A. Booij, *J. Appl. Phys.* **76**, 3835 (1994); C. B. Whan, A. B. Cawthorne, and C. J. Lobb, *Phys. Rev. B* **53**, 12 340 (1996); M. Octavio, C. B. Whan, and C. J. Lobb, *Appl. Phys. Lett.* **60**, 766 (1992); G. Filatrella, N. F. Pedersen, and K. Wiesenfeld, *ibid.* **72**, 1107 (1998); P. Hadley, M. R. Beasley, and K. Wiesenfeld, *Phys. Rev. B* **38**, 8712 (1988); Y. Braiman, W. L. Ditto, K. Wiesenfeld, and M. L. Spano, *Phys. Lett. A* **206**, 54 (1995); M. Darula, S. Beuven, M. Siegel, A. Darulova, and P. Seidel, *Appl. Phys. Lett.* **67**, 1618 (1995).
- ³A. K. Jain, K. K. Likharev, J. E. Lukens, and J. E. Sauvageau, *Phys. Rep.* **109**, 309 (1984); S. P. Benz and C. J. Burroughs, *Appl. Phys. Lett.* **58**, 2162 (1991); A. B. Cawthorne, P. Barbara, and C. J. Lobb, *IEEE Trans. Appl. Supercond.* **7**, 3403 (1997).
- ⁴P. Barbara, A. B. Cawthorne, S. V. Shitov, and C. J. Lobb, *Phys. Rev. Lett.* **82**, 1963 (1999).
- ⁵J. K. Harbaugh and D. Stroud, *Phys. Rev. B* **61**, 14 765 (2000).
- ⁶L. A. Lugiato and M. Milani, *Nuovo Cimento Soc. Ital. Fis.*, B **55**, 417 (1980); R. Bonifacio, F. Casagrande, and L. A. Lugiato, *Opt. Commun.* **36**, 159 (1981); R. Bonifacio, F. Casagrande, and G. Casati, *ibid.* **40**, 219 (1982); R. Bonifacio, F. Casagrande, and M. Milani, *Lett. Nuovo Cimento Soc. Ital. Fis.* **34**, 520 (1982).
- ⁷K. Wiesenfeld, P. Colet, and S. H. Strogatz, *Phys. Rev. Lett.* **76**, 404 (1996).
- ⁸A. B. Cawthorne, P. Barbara, S. V. Shitov, C. J. Lobb, K. Wiesenfeld, and A. Zangwill, *Phys. Rev. B* **60**, 7575 (1999).
- ⁹G. Filatrella, N. F. Pedersen, and K. Wiesenfeld, *Phys. Rev. E* **61**, 2513 (2000).
- ¹⁰F. K. Abdullaev, A. A. Abdumalikov, Jr., O. Buisson, and E. N. Tsoy, *Phys. Rev. B* **62**, 6766 (2000).
- ¹¹See, e.g., S. Teitel and C. Jayaprakash, *Phys. Rev. B* **27**, 598 (1983).
- ¹²J. C. Slater, *Microwave Electronics* (D. Van Nostrand, New York, 1950).
- ¹³A. Yariv, *Quantum Electronics*, 2nd ed. (Wiley, New York, 1975).
- ¹⁴S. Chakravarty, G.-L. Ingold, S. Kivelson, and A. Luther, *Phys. Rev. Lett.* **56**, 2303 (1986).
- ¹⁵A. O. Caldeira and A. J. Leggett, *Ann. Phys. (N.Y.)* **149**, 374 (1983); V. Ambegaokar, U. Eckern, and G. Schön, *Phys. Rev. Lett.* **48**, 1745 (1982).
- ¹⁶M. Tinkham, *Introduction to Superconductivity*, 2nd ed. (McGraw-Hill, New York, 1996).
- ¹⁷W. H. Press, S. A. Teukolsky, W. T. Vetterling, and B. P. Flannery, *Numerical Recipes* (Cambridge University Press, New York, 1992).
- ¹⁸See, e.g., M. Abramowitz and I. A. Stegun, *Handbook of Mathematical Functions* (Dover, New York, 1972), Eqs. 9.1.42–9.1.45.
- ¹⁹Y. Kuramoto, in *International Symposium on Mathematical Problems in Theoretical Physics*, edited by H. Araki, Lecture Notes in Physics Vol. 39 (Springer, Berlin, 1975), pp. 420–422.
- ²⁰See, e.g., S. H. Strogatz, *Physica D* **143**, 1 (2000); K. Wiesenfeld, P. Colet, and S. H. Strogatz, *Phys. Rev. Lett.* **76**, 404 (1996).
- ²¹B. Vasilic, P. Barbara, S. V. Shitov, E. Ott, T. M. Antonsen, and C. J. Lobb, Abstract Y27.001 of the APS March Meeting, Seattle, WA, 2001.